Food Chemistry 161 (2014) 53–59

Contents lists available at ScienceDirect

Food Chemistry

journal homepage: www.elsevier.com/locate/foodchem

Double-layered microparticles with enzyme-triggered release for the targeted delivery of water-soluble bioactive compounds to small intestine

Kyung Min Park [a], Ho Sung [b], Seung Jun Choi [c], Young Jin Choi [a,d], Pahn-Shick Chang [a,d,*]

[a] Department of Agricultural Biotechnology, Seoul National University, Seoul 151-921, Republic of Korea
[b] R&D Center, Daesang Corporation, Gyeonggi-Do 467-813, Republic of Korea
[c] Department of Food Science and Technology, Department of Interdisciplinary Bio IT Materials, Seoul National University of Science and Technology, Seoul 139-743, Republic of Korea
[d] Center for Food and Bioconvergence, Research Institute for Agriculture and Life Sciences, Seoul National University, Seoul 151-742, Republic of Korea

ARTICLE INFO

Article history:
Received 9 December 2013
Received in revised form 28 February 2014
Accepted 26 March 2014
Available online 4 April 2014

Keywords:
Enzyme-triggered release
Double-layered microparticle
Targeted delivery
In vitro digestion model
Response surface methodology

ABSTRACT

Double-layered microparticles for enzyme-triggered release in the gastrointestinal tract were prepared by spray-chilling a water/oil/water emulsion, which could be a promising candidate for the targeted delivery of water-soluble bioactive compounds. Based on response surface methodology, the optimum conditions for 2nd emulsifier content, concentration ratio of the single emulsion to the coating material, and dispersion fluid temperature were 201.5 μmol, 0.30, and 10.1 °C, respectively. Morphological characterisation using an FE-SEM indicated that double-layered microparticles with diameters of 7–10 μm were spherical and possessed scores of inner droplets. Release profiles generated using *in vitro* digestion models revealed that the core of double-layered microparticles was gradually released by enzymatic degradation when exposed to the simulated intestinal environment. The accumulative release reached 59.8 ± 0.2% within a residence time of 3 h, whereas they were resistant to gastric release-stimuli, such as extremely low pH and pepsin (below 2.4 ± 0.6%).

1. Introduction

Recent progress in molecular biology and biotechnology has led to the development of biotherapeutics and the discovery of bioactive compounds. Unfortunately, most bioactive compounds are prone to undesired inactivation or degradation under the hostile bio-environment, such as extremely low pH and enzymes in the stomach (LaVan, Lynn, & Langer, 2002). In addition, they scarcely reach their intended destination in the gastrointestinal (GI) tract, which results in low bioavailability upon oral administration (De Koker et al., 2011). These limitations have encouraged the need for high doses and/or frequent administration to obtain therapeutic efficacy, which can result in toxic and adverse effects (Almeida & Souto, 2007). Aside from high and/or frequent intakes, one approach to obtain a health benefit is to enhance the stability of bioactive compounds in the GI tract and to facilitate controlled release at the desired site for digestion and/or absorption (Augustin, Sanguansri, & Lockett, 2013; Champagne & Fustier, 2007). For this reason, technologies for encapsulation focusing on triggered carriers have been extensively investigated in drug delivery systems. For application to a targeted delivery system, biotherapeutic carriers must not only protect the inner bioactive compounds from the external environment, but should also be able to release their payload in response to certain stimuli at the target destination (Delcea, Möhwald, & Skirtach, 2011).

Among various biocompatible and biodegradable carries for controlled release, poly lactic-co-glycolic acid (PLGA, US FDA-approved for clinical use) has attracted a great deal of interest and has been utilised extensively for biomedical and pharmaceutical applications. As a drug carrier, however, PLGA has several inherent problems, such as initial-burst release and low stability against undesired release-stimuli (Emami et al., 2009; Lee, Loei, Widjaja, & Loo, 2011; Lee, Widjaja, & Loo, 2010). Furthermore, because PLGA degradation is a prerequisite for core release during the bioerosion phase, the resulting acidic microenvironment may cause inactivation or denaturation of the loaded bioactive compounds (Sinha & Trehan, 2003). Gelatinized sweet potato starch, which was used as a coating material in this study, is a natural material with greater biocompatibility and stability against undesirable release-stimuli

* Corresponding author at: Department of Agricultural Biotechnology, Seoul National University, Seoul 151-921, Republic of Korea. Tel.: +82 2 880 4852; fax: +82 2 873 5095.
E-mail address: pschnag@snu.ac.kr (P.-S. Chang).

http://dx.doi.org/10.1016/j.foodchem.2014.03.125
0308-8146/

in the stomach. In addition, it is spontaneously degraded through enzymatic hydrolysis in the small intestine, which would not lead to the acidic conditions mentioned above.

On the other hand, the size of delivery carriers is typically located either in the nanometre or micrometre range. The former size range is particularly important in parenteral administration, because only nanometre-sized delivery carriers can be utilised for the circulation system. From the patient's viewpoint, oral administration is the preferred route because it allows painless and easy self-medication, especially for chronic therapy (Plapied, Duhem, des Rieux, & Préat, 2011). Micrometre-sized carriers are attractive for such oral administration due to the prevention of aggregation and superior loading capacity (Delcea et al., 2011).

The primary aim of the present study was to prepare double-layered microparticles for oral administration of water-soluble bioactive compounds for absorption, which occurs mainly in the small intestine. To increase encapsulation efficiency, variables were optimised through response surface methodology. With regard to applications, microparticle lyophilization was performed to obtain further advantages, such as improved physiochemical stability, ease of storage, and precision of dosing (Dianawati, Mishra, & Shah, 2013; Dollo et al., 2003). The effects of pH and thermal stimuli on the stability of the double-layered microparticles were evaluated during long-term exposure, and the release profile was investigated using *in vitro* digestion models simulating the GI tract.

2. Materials and methods

2.1. Materials

Polyglycerol polyricinoleate (PGPR) and Tween 60 (polyoxyethylene 20 sorbitan monostearate) were supplied by Ilshinwells (Seoul, Korea). Fully hydrogenated canola oil (FHCO) was a kind gift from Lotte Samkang Co., Ltd. (Seoul, Korea). Sweet potato starch (SPS) was purchased from Wako Pure Chemical Industries, Ltd. (Osaka, Japan). Enzymes (pepsin, pancreatin, and lipase) for simulating *in vitro* digestion models were purchased from Sigma–Aldrich Co. (Milwaukee, WI). All other chemicals were of reagent grade and were used without further purification.

2.2. Preparation of double-layered microparticles

Double-layered microparticles were prepared by the spray-chilling method after formation of a double emulsion. Briefly, deionized distilled water (internal aqueous phase, core solution) was added to FHCO (oil phase, wall material) containing 20 μM PGPR (referred to as the 1st emulsifier, with a low hydrophilic–lipophilic balance) to achieve a volumetric ratio of 0.6 ([core solution]/[wall material]). The single emulsion (water-in-oil) was formed by homogenization at 8000 rpm for 60 s with an Ultra-Turrax T25 dispersion unit (Ika Werke GmbH & Co., Staufen, Germany). This primary emulsion was immediately injected into a gelatinized solution (external aqueous phase, coating material) consisting of 16% SPS and 30% isomalt at the desired ratio ([single emulsion]/[coating material]). The mixture was then homogenised under the same conditions as in the 1st emulsification at the designated concentrations of Tween 60 (referred to as the 2nd emulsifier with a high hydrophilic–lipophilic balance) to fabricate the double emulsion (water/oil/water). The resulting double emulsion was sprayed into a dispersion fluid (0.025% polyethylene sorbitan tristearate dissolved in distilled water) using an airless spray gun (Wagner Spray Tech. Co., Baden-Württemberg, Germany). Dried double-layered microparticles were obtained by lyophilizing the double-emulsion microcapsules, and were stored at 4 °C for the further study.

2.3. Encapsulation efficiency

Encapsulation efficiency was determined according to the spectrophotometric method reported in our previous study with slight modifications (Chang, Lee, & Lee, 2005). Briefly, Oil red O, as an internal marker, was dissolved in FHCO (wall material) prior to the 1st emulsification and then isolated from the external solvent and was quantitatively analysed using a spectrophotometer after microencapsulation. Before lyophilization, 10 ml of *n*-hexane was added to 20 ml of the dispersion containing the double-emulsion microcapsules. This mixture was incubated for 10 min with magnetic stirring at 500 rpm to extract free FHCO and then allowed to stand until separation. The supernatant from the mixture was collected for UV–visible spectrophotometric analysis. The absorbance at 510 nm (λ_{max} of Oil red O) was proportional to the amount of Oil red O (data not shown), which directly reflects the amount of free FHCO excluded from microencapsulation. Encapsulation efficiency was defined as microencapsulation yield (%), which was calculated from the following Eq. (1):

$$\text{Microencapsulation yield } (\%) = \frac{\text{the amount of FHCO actually loaded}}{\text{the initial amount of FHCO added}} \times 100 \quad (1)$$

2.4. Experimental design and statistical analysis

Response surface methodology (RSM) was performed to optimise the conditions for encapsulation. Central composite design was employed to evaluate the effects of Tween 60 content (2nd emulsifier for water/oil/water emulsion), the concentration ratio of the single emulsion to the external aqueous phase ([single emulsion]/[coating material]), and the temperature of the dispersion fluid. The design scheme consisted of 20 treatments with six central points, 2^3 cube points, and six axial points. A quadratic model for predicting the maximum point was used to describe the response of microencapsulation yield, Y, using the following Eq. (2):

$$Y = \beta_0 + \sum_{i=1}^{3}\beta_i X_i + \sum_{i=1}^{3}\beta_{ii} X_i^2 + \sum_{i=1}^{2}\sum_{j=i+1}^{3}\beta_{ij} X_i X_j \quad (2)$$

where β_0, β_i, β_{ii}, and β_{ij} are regression coefficients, and X_i and X_j represent independent variables assigned to 2nd emulsifier (Tween 60) content (X_1), [single emulsion]/[coating material] (X_2), and dispersion-fluid temperature (X_3). Five levels of each variable (X_1, 50–250 μmol; X_2, 0.1–0.5; X_3, 5–25 °C) were used in the experimental design. The units and the actual and coded levels of the independent variables are presented in Supplementary Data (Table S1). Statistical analysis was performed using Design Expert software (Stat-Ease, Minneapolis, MN).

2.5. Morphology

Morphological characterisation of the dried double-layered microparticles was performed using a combined focused ion beam (FIB) with field-emission scanning electron microscopy (FE-SEM) (Carl Zeiss AG, Weimar, Germany). Microparticles were attached to SEM stubs using two-sided adhesive carbon tape to observe the external morphology. The internal structure of the microparticles was investigated by combined FIB milling and FE-SEM. For milling, the sample was tilted to 45° and ion milling was performed perpendicular to the sample surface, as the electron beam hit the surface at an angle. Imaging was obtained using both the ion beam and the electron beam to control sample positioning and to adjust the FIB/SEM confocal point. The Ga^+ ions of the FIB

were accelerated at 30 kV. In all cases, the SEM was operated with a working distance of 5 mm and acceleration voltage of 5-kV.

2.6. Storage stability

The storage stability of the double-layered microparticles was evaluated under various temperature and pH conditions. The effect of pH on microparticle stability was examined from pH 2.0 to 12.0 at a fixed temperature of 20 °C. Thermal stability was tested at temperatures of 4–60 °C at pH 7.0. Storage stability was then determined by calculating the residual amount of microparticles during long-term incubation under the designed conditions.

2.7. In vitro release profile

An *in vitro* digestion model simulating the gastrointestinal tract in humans was employed to investigate the release profile of double-layered microparticles, which was a slight modification of the method described by Versantvoort, Oomen, Van de Kamp, Rompelberg, and Sips (2005). The *in vitro* digestion process was simulated in a simplified manner by applying physiologically based conditions i.e. chemical composition of digestive fluids, environmental pH, and residence periods for each compartment. Although part of the digestive process occurs in the oral cavity due to salivary amylase, the *in vitro* model describes a two-step procedure simulating processes in the stomach and small intestine, as these compartments are most likely to determine bioaccessibility (Washington & Wilson, 2001). The large intestinal tract was not considered, as digestion and absorption of bioactive compounds mainly takes place in the small intestine. The *in vitro* model simulated digestive processes in the human gastrointestinal tract under fasting conditions. The biomimetic model is shown in Supplementary Data (Table S2). Briefly, the digestive juices were pre-incubated at 37 ± 0.5 °C for 15 min prior to the addition of samples. Then double-layered microparticles were injected into the digestive juices and incubated at 37 °C for 180 min (typical residence period) with orbital shaking. Subsequently, aliquots at intervals of 30 min were analysed to evaluate the cumulative release (%) of the core. All of the release experiments were performed in triplicate.

3. Results and discussion

3.1. Optimising microencapsulation and model verification

Microencapsulating conditions including 2nd emulsifier content, [single emulsion]/[coating material], and dispersion fluid temperature were optimised for maximum encapsulation efficiency. Central composite experimental design and the corresponding response values are shown in Table 1. A second-order polynomial model describing the correlation between the microencapsulation yield and the three independent variables was obtained by statistical analysis, as shown in Eq. (3):

$$Y = 32.83 + 0.36X_1 + 167.00X_2 + 2.08X_3 - 0.0014X_1^2 - 228.75X_2^2 - 0.13X_3^2 + 0.06X_1X_2 + 0.01X_1X_3 - 4.50X_2X_3 \quad (3)$$

Each of the observed values was compared with the predicted value, which was calculated with model Eq. (3) (Table 1). The statistical significance of Eq. (3), confirmed by analysis of variance, is shown in Table 2. The effects of variables as linear, quadratic, or interaction coefficients on the response, were tested for adequacy. The fit value, the coefficient of multiple determination of the second-order polynomial model (termed R^2), was 0.9578, which indicated that the fitted model could explain 95.78% of the variability in the response. The coefficient of variation (CV = 3.21%) was less than 5%, indicating good precision and reliability of the experiments, and showing that the model was reproducible. The *P*-value for the model in Table 2 showed that the model was significant ($P < 0.01$), and the *P*-value for the lack of fit indicated significance. As shown in Table 1, all three independent variables had significant linear and quadratic effects ($P < 0.01$) on the microencapsulation yield. The interaction effects among the three independent variables were not significant, with the exception of an interaction between the 2nd emulsifier concentration, and dispersion-fluid temperature (*P*-values of $X_1X_2 = 0.7965$, $X_1X_3 = 0.0094$, and $X_2X_3 = 0.0554$).

Table 1
Experimental conditions of the central composite design for microencapsulation optimisation.

Run no.	Variables			Response (%)	
	X_1	X_2	X_3	Predicted	Observed
1	100 (−1)	0.2 (−1)	10 (−1)	91.80	90.0 ± 0.33
2	200 (1)	0.2 (−1)	10 (−1)	98.93	94.0 ± 1.41
3	100 (−1)	0.4 (1)	10 (−1)	90.40	89.9 ± 0.78
4	200 (1)	0.4 (1)	10 (−1)	97.53	98.5 ± 0.49
5	100 (−1)	0.2 (−1)	20 (1)	79.43	78.3 ± 0.45
6	200 (1)	0.2 (−1)	20 (1)	99.85	99.1 ± 0.05
7	100 (−1)	0.4 (1)	20 (1)	69.03	72.7 ± 0.66
8	200 (1)	0.4 (1)	20 (1)	89.45	91.1 ± 1.61
9	50 (−2)	0.3 (0)	15 (0)	70.28	69.8 ± 3.27
10	250 (2)	0.3 (0)	15 (0)	97.83	99.0 ± 0.21
11	150 (0)	0.1 (−2)	15 (0)	95.35	99.3 ± 0.28
12	150 (0)	0.5 (2)	15 (0)	83.55	80.3 ± 1.07
13	150 (0)	0.3 (0)	5 (−2)	96.33	99.1 ± 0.26
14	150 (0)	0.3 (0)	25 (2)	75.88	73.8 ± 1.28
15	150 (0)	0.3 (0)	15 (0)	98.60	98.8 ± 0.17
16	150 (0)	0.3 (0)	15 (0)	98.60	98.8 ± 0.05
17	150 (0)	0.3 (0)	15 (0)	98.60	98.4 ± 0.05
18	150 (0)	0.3 (0)	15 (0)	98.60	98.7 ± 0.08
19	150 (0)	0.3 (0)	15 (0)	98.60	98.6 ± 0.09
20	150 (0)	0.3 (0)	15 (0)	98.60	99.0 ± 0.12

X_1, 2nd emulsifier content (μmol).
X_2, [single emulsion]/[coating material].
X_3, dispersion-fluid temperature (°C).

Table 2
Analysis of variance (ANOVA) of the second-order response surface model.

Source	Degree of freedom	Sum of square	Mean squares	*F*-value	*P*-value
Model	9	1956.21	217.357	25.21	<0.0001
Linear	3	1316.44	438.815	50.90	<0.0001
X_1	1	759.00	759.00	88.04	<0.0001
X_2	1	139.24	139.24	16.15	0.0024
X_3	1	418.20	418.20	48.51	<0.0001
Quadratic	3	510.22	170.073	19.73	0.008
X_1^2	1	332.68	332.68	38.59	<0.0001
X_2^2	1	131.56	131.56	15.26	0.0029
X_3^2	1	245.54	245.54	28.48	0.0003
Interaction	3	129.55	43.183	5.01	0.023
X_1X_2	1	0.61	0.61	0.070	0.7965
X_1X_3	1	88.45	88.45	10.26	0.0094
X_2X_3	1	40.50	40.50	4.70	0.0554
Residual	10	86.21	8.62		
Lack of fit	5	86.01	17.20	412.83	<0.0001
Pure error	5	0.21	0.042		
Corrected total	19	2042.43			

$R^2 = 0.9578$.
Adj $R^2 = 0.9198$.
CV: 3.21%.
Adequate precision ratio = 14.847.
For the identification of X_1, X_2, and X_3, refer to Table 1.

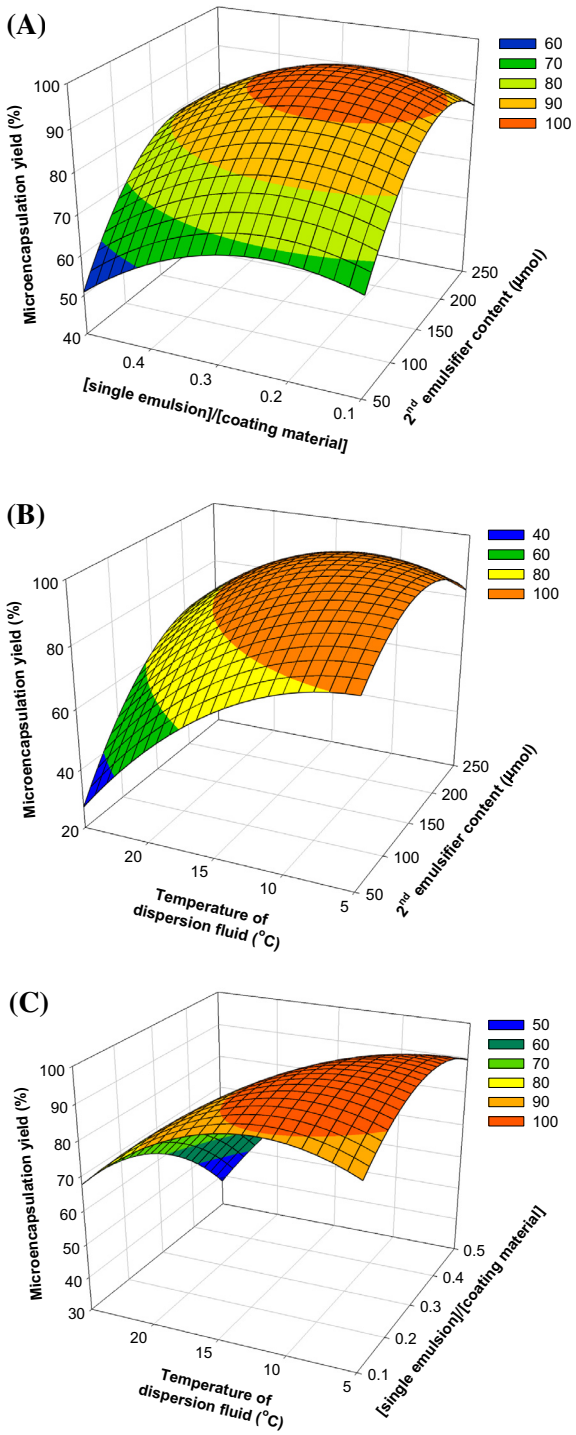

Fig. 1. Response surface plots showing the effects of variables on microencapsulation yield. (A) Effects of 2nd emulsifier content and the [single-emulsion]/[coating material] ratio in dispersion fluid at a temperature of 10 °C. (B) Effects of 2nd emulsifier content and dispersion fluid temperature at a [single-emulsion]/[coating material] ratio of 0.3. (C) Effects of [single-emulsion]/[coating material] ratio and dispersion fluid temperature at a 2nd emulsifier concentration of 100 μmol.

Fig. 1 shows the effects of the independent variables on the microencapsulation yield. Fig. 1A shows the effects of 2nd emulsifier content and [single emulsion]/[coating material] on microencapsulation yield at a 15 °C dispersion temperature. When [single emulsion]/[coating material] was constant, microencapsulation yield increased with increases in 2nd emulsifier content. At constant 2nd emulsifier content, microencapsulation yield did not change significantly with increases in [single-emulsion]/[coating material], indicating that 2nd emulsifier content was the most effective factor for maximising microencapsulation yield. The effects of 2nd emulsifier content and dispersion-fluid temperature on microencapsulation yield at a constant [single emulsion]/[coating material] of 0.3 are shown in Fig. 1B. An increase in 2nd emulsifier concentration and a reduction in temperature resulted in increased microencapsulation yield. However, microencapsulation yield did not increase further above the optimum 2nd emulsifier concentration (approx. 150 μmol, and below the optimum temperature of the dispersion fluid (approx. 15 °C). Fig. 1C shows the effects of the [single emulsion]/[coating material] ratio and dispersion-fluid temperature on microencapsulation yield at a 2nd emulsifier concentration of 150 μmol. The increases in both dispersion-fluid temperature and [single emulsion]/[coating material] ratio decreased microencapsulation yield.

Based on these results, the optimum 2nd emulsifier content, [single emulsion]/[coating material], and dispersion-fluid temperature were found to be 201.5 μmol, 0.3, and 10.1 °C, respectively. The predicted microencapsulation yield was 100.5%, whereas the actual microencapsulation yield under the conditions optimised in this study was 98.1 ± 0.54%. The actual microencapsulation yield was not significantly different from the predicted value, thus verifying the validity of the designed model.

3.2. Morphological characterisation

In targeted delivery systems, the characteristics of microcapsules, such as the retention of bioactive compounds in the core, protection from undesired disruption, and controlled release by external stimuli, are significantly influenced by their size distribution, surface morphology, and internal structure (Acharya et al., 2010; Lee et al., 2011; Singh, Hemant, Ram, & Shivakumar, 2010). To confirm the formation of double-emulsion microcapsules by spray-chilling, optical microscopy was performed prior to lyophilization. Optical microscopic images indicated that the morphology of microcapsules with diameters of 7–10 μm was a spherical, double-layered shape containing inner droplets (Fig. 2A). The powdered microparticles through lyophilization were cross-sectioned using the FIB method to study their internal structure. The advantage of FIB cross-sectioning is that it can be performed under permanent SEM control, and the Ga^+-ion beam produces a smooth cross-section in the submicrometre range. As shown in Fig. 2B, lyophilized microparticles retained a spherical shape with double layers, and had fairly smooth surfaces, indicating that freeze-drying could be applied to the dehydration process of double-emulsion microcapsules. The surface of the double-layered microparticles had some dimples and wrinkles, which was presumed to occur during lyophilization due to uneven dehydration from the external surface of wall material, consisting of gelatinized SPS and isomalt. This morphological phenomenon has been commonly reported in various studies on other spray-dried microcapsules based on carbohydrates, proteins, or polyelectrolytes (Danviriyakul, McClements, Decker, Nawar, & Chinachoti, 2002; Simovic et al., 2010; Tan, Simovic, Davey, Rades, & Prestidge, 2009; Zhong & Jin, 2009). Although the internal structure was not uniform, the double-layered microparticles possessed scores of inner droplets with diameters of 0.5–1.0 μm. In addition, the thickness of the external wall surrounding the inner droplets was approximately 0.3–0.5 μm based on FE-SEM images.

3.3. Stability on pH and thermal stimuli

The storage stability of microparticles produced under the optimum conditions was evaluated under various pH and temperature

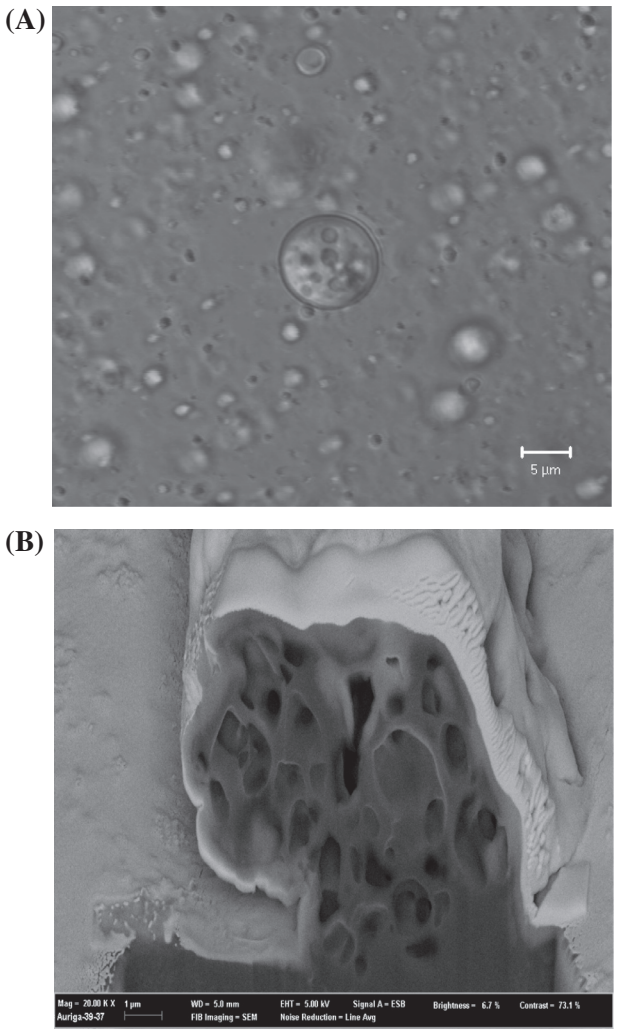

Fig. 2. Optical microscopic (A) and field-emission scanning electron microscopy (FE-SEM) (B) images showing the morphology and internal structure of double-layered microparticles.

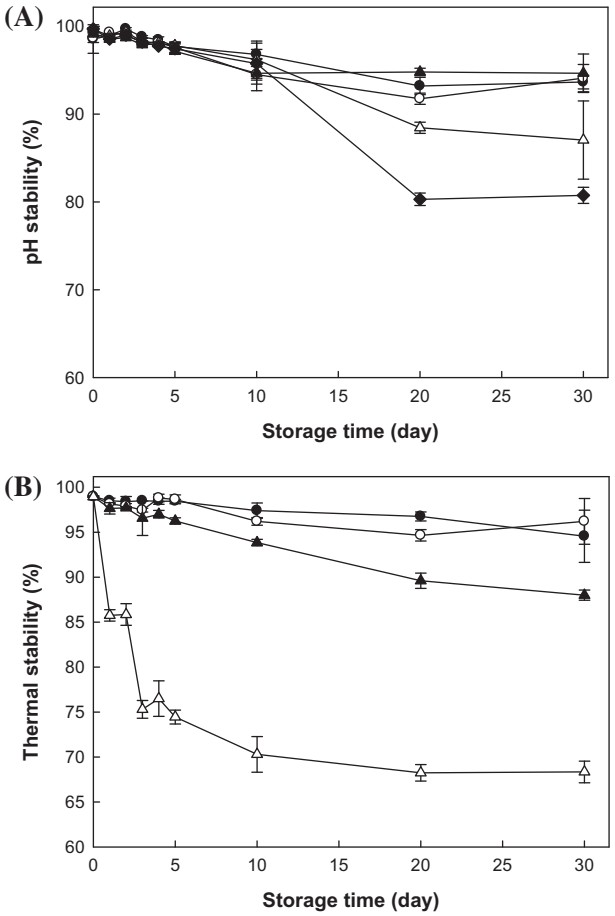

Fig. 3. Effects of pH and temperature on storage stability of double-layered microparticles. (A) pH stability (●, pH 2.0; ○, pH 4.5; ▲, pH 7.0; △, pH 9.5; ♦, pH 12.0). (B) Thermal stability (●, 4 °C; ○, 20 °C; ▲, 40 °C; △, 60 °C).

conditions. Variation in stability as a function of pH is shown in Fig. 3A. With 10 days of incubation, microparticles remained very stable and maintained almost 94.5% of their stability over the entire pH range tested. However, samples stored at different pHs had a different stability after 20 days of incubation. At 30 days of incubation, the pH stability leveled off to 87.1% and 80.9% for microparticles incubated at pH 9.0 and 12.0, respectively, whereas those at pH 2.0, 4.5, and 7.0 showed a relatively high stability of over 93.7%.

These results indicating that the stability of microparticles exposed to alkaline pH was relatively low as compared with acidic pH, and can be explained as follows. First, the coating material containing gelatinized SPS could be partially cleaved by the action so-called β-elimination. This phenomenon, i.e., β-elimination of polysaccharides, is generally considered to be accelerated in alkaline pH (Fujisawa, Isogai, & Isogai, 2010; Knill & Kennedy, 2003; Pavasars, Hagberg, Borén, & Allard, 2003). Second, the high solubility of starch under alkaline conditions may be due to its enhanced hydrophilic character and partial gelatinization (Olayide, 2004). During storage under alkaline conditions, the coating material may have solubilised to some extent for the reasons described above, resulting in exposure of the inner droplets. After a certain storage period, the coating material did not completely cover all of the inner droplets. The coating material-depleted patches on the microparticles may have promoted the loss of the core solution containing bioactive compounds.

Thermal stability of microparticles was investigated by incubation at temperatures of 4–60 °C, at a fixed pH of 7.0. All samples, with the exception of those stored at 60 °C, showed relatively high stability over the 30-day storage period. The thermal stabilities of microcapsules stored at 4, 20, and 40 °C were well maintained at over 88.0% during the entire incubation period. However, incubation at 60 °C reduced the stability of microparticles from the first day of initial incubation. The low stability of microparticles at relatively high temperatures could be due to the melting temperature of FHCO used as the wall material. According to the supplier, the melting point of FHCO is 60–70 °C. The stability of microparticles decreased to 68.4% after storage for 30 days when the temperature was near the melting point of the wall material (FHCO). The storage of microparticles at around the melting temperature of FHCO may have partially liquefied the wall material, thus decreasing the thermal stability of microparticles. Therefore, the core solution may have rapidly spilled out when the wall material melted at the high temperature. Conversely, solidification of FHCO, as a result of fat crystallization at room temperature, may prevent leakage of the core solution containing bioactive compounds, by reducing oil droplet coalescence (McClements, 2005). The negligible losses of the core incubated at both 4 and 20 °C were below 5.4%, which suggested that the double-layered microparticles could efficiently retain the core during storage at a refrigerating temperature or even at room temperature. In terms of controlled release, high stability over wide ranges of pH and temperature reflect that the

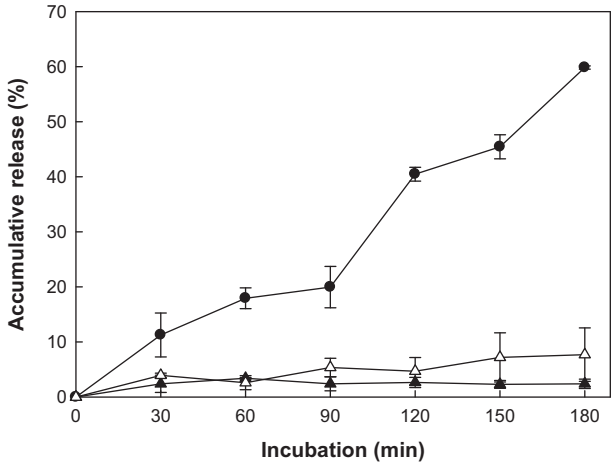

Fig. 4. Release profiles of the core from double-layered microparticles under the *in vitro* digestion models (●, intestinal; ▲, gastric; △, deionized distilled water).

double-layered microparticles would be highly resistant to undesired release-stimuli in the GI tract.

3.4. In vitro release profile in simulated digestion models

The *in vitro* release properties of double-layered microparticles prepared under the conditions optimised through RSM were investigated in simulated gastric (pH 2.0) and intestinal environments (pH 7.8). Generally, to be useful as a delivery carrier for intestinal absorption, microcapsules should protect bioactive compounds in the core from both acidic and enzymatic degradation when exposed to the gastric environment (Gaucher, Satturwar, Jones, Furtos, & Leroux, 2010). That is, coating and/or wall materials should be tolerant of gastric release-stimuli, such as extremely low pH and pepsin secreted from the stomach. In contrast, once the microcapsule reaches the small intestine, it should release the core from the matrix in a sustained manner (Anal & Singh, 2007; Rekha & Sharma, 2009). As shown in Fig. 4, approximately 2.4% of the core was released from the double-layered microparticles over 3 h when incubated in a simulated gastric juice, which was not significantly different from the release profile of the blank test in deionized distilled water. The time course of release indicated that the double-layered microparticles effectively protected the core against gastric release-stimuli, that is to say, they had a stubborn resistance to degradation by gastric acid and enzymes. These observations are consistent with the results of stability experiments under acidic pH. In contrast to what happens in the gastric environment, the core was released from the double-layered microparticles in proportion to the incubation time, when exposed to a simulated intestinal environment with duodenal juice, and the cumulative release of core increased up to 60.1% at 3 h from the initial incubation. The release profile triggered by intestinal stimuli was likely due to stepwise degradation, namely, enzymatic hydrolysis of coating and wall materials of the double-layered microparticles. In theory, pancreatin, an enzyme complex containing β-amylase, has the ability to hydrolyse the glycosidic bonds of gelatinized SPS used in the coating material, resulting in exposure of the wall material. As a result, coating material-depleted patches on the microparticles could be easily accessed by intestinal lipases. Subsequently, the enzymatic degradation of the wall material led to release of the core.

It has been regarded that release kinetics is one of key considerations in drug delivery systems (Costache, Qu, Ducheyne, & Devore, 2010; Yang, Chung, & Ping Ng, 2001). Especially, it has frequently been posed that the initial burst, which refers to the early rapid release, may cause an overdose resulting in serious toxicity within the body (Ahmed, Elkharraz, Irfan, & Bodmeier, 2012; Huang, Chestang, & Brazel, 2002; Riaz Ahmed, Ciper, & Bodmeier, 2010; Thote, Chappell, Kumar, & Gupta, 2005). In addition, such microparticles tend to have a very slow release period, the so-called lag time, after the initial burst (Huang et al., 2002; Wang, Wang, & Schwendeman, 2002). As shown in Fig. 4, release kinetics of the double-layered microparticles showed a near zero-order release, with no initial burst. This phenomenon, i.e., a release profile without an initial burst, can be assumed to principally occur due to stepwise degradation of the double-layered microparticles, as mentioned above. On the other hand, when exposed to the intestinal environment, certain components within bile salts can be adsorbed onto the microparticle surface (Mun, Decker, & McClements, 2007). These components could displace some of the original emulsifier (Tween 60 in the present study) from the microparticle surface. Such displacement of emulsifiers would result in changes in oil droplet size and accessibility of lipid-degraded enzymes to oil droplets. Actually, the extent of the change in oil droplet size could vary depending on the lipid state. Liquid state oil droplets in an emulsion could be easily broken down to smaller droplets by bile salts, resulting in an increased surface area. An increase in surface area results in an expanded interface between enzymes and substrates, i.e., easy access of lipase, which could lead to an initial burst release of the core. However, FHCO, which was used as the wall material in this study, was in a solid state at physiological temperature. Therefore, the breakdown of inner droplets, including FHCO, and accessibility of enzymes may not be as easy as in microparticles consisting of liquid-state oil, which may suppress the initial burst release. Thus, the core of the double-layered microparticles, produced in this study, could be gradually released without an initial burst in the simulated intestinal environment.

4. Conclusions

Double-layered microparticles for smart delivery of water-soluble bioactive compounds were prepared by the spray-chilling method after formation of a double emulsion. To increase the efficiency of encapsulation, optimum conditions for producing double-layered microparticles were identified by RSM. The variables, such as 2nd emulsifier content, [single emulsion]/[coating material], and dispersion-fluid temperature, significantly influenced the encapsulation efficiency, and the optimum conditions for maximum yield were as follows: 201.5 μmol of the 2nd emulsifier, [single emulsion]/[coating material] ratio of 0.3, and dispersion-fluid temperature of 10.1 °C. Morphological characterisation was performed to identify the internal structure using FE-SEM combined with FIB, which revealed that the microparticles were 7–10 μm in diameter, with spherical double-layered microcapsules containing inner droplets. In the experiments to determine the release profile using *in vitro* digestion models, double-layered microparticles gradually released the core without an initial burst when exposed to the intestinal environment, and showed negligible loss of the core in the gastric environment. These results suggested that double-layered microparticles could be used as a novel carrier for intestinal absorption and that the encapsulation technique could be applied to smart delivery systems for various water-soluble bioactive compounds.

Acknowledgements

This work was financially supported in part by Basic Science Research Program through the National Research Foundation of Korea (NRF) funded by the Ministry of Education

(NRF-2011-0010786), and by High Value-added Food Technology Development Program (313021-3) by the Ministry of Agriculture, Food and Rural Affairs, Republic of Korea.

Appendix A. Supplementary data

Supplementary data associated with this article can be found, in the online version, at http://dx.doi.org/10.1016/j.foodchem.2014.03.125.

References

Acharya, G., Shin, C. S., Vedantham, K., McDermott, M., Rish, T., Hansen, K., et al. (2010). A study of drug release from homogeneous PLGA microstructures. *Journal of Controlled Release, 146*(2), 201–206.

Ahmed, A. R., Elkharraz, K., Irfan, M., & Bodmeier, R. (2012). Reduction in burst release after coating poly(D, L-lactide-co-glycolide) (PLGA) microparticles with a drug-free PLGA layer. *Pharmaceutical Development and Technology, 17*(1), 66–72.

Almeida, A. J., & Souto, E. (2007). Solid lipid nanoparticles as a drug delivery system for peptides and proteins. *Advanced Drug Delivery Reviews, 59*(6), 478–490.

Anal, A. K., & Singh, H. (2007). Recent advances in microencapsulation of probiotics for industrial applications and targeted delivery. *Trends in Food Science & Technology, 18*(5), 240–251.

Augustin, M. A., Sanguansri, L., & Lockett, T. (2013). Nano- and micro-encapsulated systems for enhancing the delivery of resveratrol. *Annals of the New York Academy of Sciences, 1290*(1), 107–112.

Champagne, C. P., & Fustier, P. (2007). Microencapsulation for the improved delivery of bioactive compounds into foods. *Current Opinion in Biotechnology, 18*(2), 184–190.

Chang, P.-S., Lee, J. H., & Lee, J. H. (2005). Development of a new colorimetric method determining the yield of microencapsulation of α-tocopherol. *Journal of Agricultural and Food Chemistry, 53*(19), 7385–7389.

Costache, M. C., Qu, H., Ducheyne, P., & Devore, D. I. (2010). Polymer–xerogel composites for controlled release wound dressings. *Biomaterials, 31*(24), 6336–6343.

Danviriyakul, S., McClements, D. J., Decker, E., Nawar, W. W., & Chinachoti, P. (2002). Physical stability of spray-dried milk fat emulsion as affected by emulsifiers and processing conditions. *Journal of Food Science, 67*(6), 2183–2189.

De Koker, S., De Cock, L. J., Rivera-Gil, P., Parak, W. J., Auzély Velty, R., Vervaet, C., et al. (2011). Polymeric multilayer capsules delivering biotherapeutics. *Advanced Drug Delivery Reviews, 63*(9), 748–761.

Delcea, M., Möhwald, H., & Skirtach, A. G. (2011). Stimuli-responsive LbL capsules and nanoshells for drug delivery. *Advanced Drug Delivery Reviews, 63*(9), 730–747.

Dianawati, D., Mishra, V., & Shah, N. P. (2013). Effect of drying methods of microencapsulated *Lactobacillus acidophilus* and *Lactococcus lactis* ssp. cremoris on secondary protein structure and glass transition temperature as studied by Fourier transform infrared and differential scanning calorimetry. *Journal of Dairy Science, 96*(3), 1419–1430.

Dollo, G., Le Corre, P., Guérin, A., Chevanne, F., Burgot, J. L., & Leverge, R. (2003). Spray-dried redispersible oil-in-water emulsion to improve oral bioavailability of poorly soluble drugs. *European Journal of Pharmaceutical Sciences, 19*(4), 273–280.

Emami, J., Hamishehkar, H., Najafabadi, A. R., Gilani, K., Minaiyan, M., Mahdavi, H., et al. (2009). A novel approach to prepare insulin-loaded poly(lactic-co-glycolic acid) microcapsules and the protein stability study. *Journal of Pharmaceutical Sciences, 98*(5), 1712–1731.

Fujisawa, S., Isogai, T., & Isogai, A. (2010). Temperature and pH stability of cellouronic acid. *Cellulose, 17*(3), 607–615.

Gaucher, G., Satturwar, P., Jones, M.-C., Furtos, A., & Leroux, J.-C. (2010). Polymeric micelles for oral drug delivery. *European Journal of Pharmaceutics and Biopharmaceutics, 76*(2), 147–158.

Huang, X., Chestang, B. L., & Brazel, C. S. (2002). Minimization of initial burst in poly(vinyl alcohol) hydrogels by surface extraction and surface-preferential crosslinking. *International Journal of Pharmaceutics, 248*(1–2), 183–192.

Knill, C. J., & Kennedy, J. F. (2003). Degradation of cellulose under alkaline conditions. *Carbohydrate Polymers, 51*(3), 281–300.

LaVan, D. A., Lynn, D. M., & Langer, R. (2002). Moving smaller in drug discovery and delivery. *Nature Reviews Drug Discovery, 1*(1), 77–84.

Lee, W. L., Loei, C., Widjaja, E., & Loo, S. C. J. (2011). Altering the drug release profiles of double-layered ternary-phase microparticles. *Journal of Controlled Release, 151*(3), 229–238.

Lee, W. L., Widjaja, E., & Loo, S. C. J. (2010). One-step fabrication of triple-layered polymeric microparticles with layer localization of drugs as a novel drug-delivery system. *Small, 6*(9), 1003–1011.

McClements, D. J. (2005). *Food emulsions: principles, practice, and techniques* (2nd ed.). Boca Raton, FL: CRC Press.

Mun, S., Decker, E. A., & McClements, D. J. (2007). Influence of emulsifier type on in vitro digestibility of lipid droplets by pancreatic lipase. *Food Research International, 40*(6), 770–781.

Olayide, S. L. (2004). Succinyl and acetyl starch derivatives of a hybrid maize: physicochemical characteristics and retrogradation properties monitored by differential scanning calorimetry. *Carbohydrate Research, 339*(16), 2673–2682.

Pavasars, I., Hagberg, J., Borén, H., & Allard, B. (2003). Alkaline degradation of cellulose: Mechanisms and kinetics. *Journal of Polymers and the Environment, 11*(2), 39–47.

Plapied, L., Duhem, N., des Rieux, A., & Préat, V. (2011). Fate of polymeric nanocarriers for oral drug delivery. *Current Opinion in Colloid & Interface Science, 16*(3), 228–237.

Rekha, M. R., & Sharma, C. P. (2009). Synthesis and evaluation of lauryl succinyl chitosan particles towards oral insulin delivery and absorption. *Journal of Controlled Release, 135*(2), 144–151.

Riaz Ahmed, A., Ciper, M., & Bodmeier, R. (2010). Reduction in burst release from poly(D, L-lactide-Co-glycolide) microparticles by solvent treatment. *Letters in Drug Design & Discovery, 7*(10), 759–764.

Simovic, S., Hui, H., Song, Y., Davey, A. K., Rades, T., & Prestidge, C. A. (2010). An oral delivery system for indomethicin engineered from cationic lipid emulsions and silica nanoparticles. *Journal of Controlled Release, 143*(3), 367–373.

Singh, M., Hemant, K., Ram, M., & Shivakumar, H. (2010). Microencapsulation: A promising technique for controlled drug delivery. *Research in Pharmaceutical Sciences, 5*(2), 65–77.

Sinha, V. R., & Trehan, A. (2003). Biodegradable microspheres for protein delivery. *Journal of Controlled Release, 90*(3), 261–280.

Tan, A., Simovic, S., Davey, A. K., Rades, T., & Prestidge, C. A. (2009). Silica-lipid hybrid (SLH) microcapsules: A novel oral delivery system for poorly soluble drugs. *Journal of Controlled Release, 134*(1), 62–70.

Thote, A. J., Chappell, J. T., Kumar, R., & Gupta, R. B. (2005). Reduction in the initial-burst release by surface crosslinking of PLGA microparticles containing hydrophilic or hydrophobic drugs. *Drug Development and Industrial Pharmacy, 31*(1), 43–57.

Versantvoort, C. H. M., Oomen, A. G., Van de Kamp, E., Rompelberg, C. J. M., & Sips, A. J. A. M. (2005). Applicability of an in vitro digestion model in assessing the bioaccessibility of mycotoxins from food. *Food and Chemical Toxicology, 43*(1), 31–40.

Wang, J., Wang, B. M., & Schwendeman, S. P. (2002). Characterization of the initial burst release of a model peptide from poly(D, L-lactide-co-glycolide) microspheres. *Journal of Controlled Release, 82*(2–3), 289–307.

Washington, N., Wilson, C., & Wilson, C. G. (2001). *Physiological pharmaceutics: Barriers to drug absorption*. Taylor & Francis.

Yang, Y.-Y., Chung, T.-S., & Ping Ng, N. (2001). Morphology, drug distribution, and in vitro release profiles of biodegradable polymeric microspheres containing protein fabricated by double-emulsion solvent extraction/evaporation method. *Biomaterials, 22*(3), 231–241.

Zhong, Q., & Jin, M. (2009). Nanoscalar structures of spray-dried zein microcapsules and in vitro release kinetics of the encapsulated lysozyme as affected by formulations. *Journal of Agricultural and Food Chemistry, 57*(9), 3886–3894.